Structure of the human MTERF4–NSUN4 protein complex that regulates mitochondrial ribosome biogenesis

Henrik Spåhr[a], Bianca Habermann[a], Claes M. Gustafsson[b], Nils-Göran Larsson[a,1], and B. Martin Hallberg[c,d,1]

[a]Department of Mitochondrial Biology, Max Planck Institute for Biology of Ageing, D-50931 Cologne, Germany; [b]Institute of Biomedicine, University of Gothenburg, S-405 30 Gothenburg, Sweden; [c]Department of Cell and Molecular Biology, Karolinska Institutet, S-171 77 Stockholm, Sweden; and [d]Centre for Structural Systems Biology, DESY-Campus, D-22603 Hamburg, Germany

Edited* by Roger D. Kornberg, Stanford University School of Medicine, Stanford, CA, and approved August 13, 2012 (received for review June 22, 2012)

Proteins crucial for the respiratory chain are translated by the mitochondrial ribosome. Mitochondrial ribosome biogenesis is therefore critical for oxidative phosphorylation capacity and disturbances are known to cause human disease. This complex process is evolutionary conserved and involves several RNA processing and modification steps required for correct ribosomal RNA maturation. We recently showed that a member of the mitochondrial transcription termination factor (MTERF) family of proteins, MTERF4, recruits NSUN4, a 5-methylcytosine RNA methyltransferase, to the large ribosomal subunit in a process crucial for mitochondrial ribosome biogenesis. Here, we describe the 3D crystal structure of the human MTERF4–NSUN4 complex determined to 2.9 Å resolution. MTERF4 is composed of structurally repeated MTERF–motifs that form a nucleic acid binding domain. NSUN4 lacks an N- or C-terminal extension that is commonly used for RNA recognition by related RNA methyltransferases. Instead, NSUN4 binds to the C-terminus of MTERF4. A positively charged surface forms an RNA binding path from the concave to the convex side of MTERF4 and further along NSUN4 all of the way into the active site. This finding suggests that both subunits of the protein complex likely contribute to RNA recognition. The interface between MTERF4 and NSUN4 contains evolutionarily conserved polar and hydrophobic amino acids, and mutations that change these residues completely disrupt complex formation. This study provides a molecular explanation for MTERF4-dependent recruitment of NSUN4 to ribosomal RNA and suggests a unique mechanism by which other members of the large MTERF-family of proteins can regulate ribosomal biogenesis.

mitochondria | translation | X-ray crystallography

Deficient oxidative phosphorylation is heavily implicated in human disease and aging and this has led to a surge in the interest to understand underlying molecular mechanisms (1). Regulation of mitochondrial DNA (mtDNA) expression is of key importance for control of oxidative phosphorylation capacity because mtDNA encodes 13 essential subunits of the respiratory chain and the ATP synthase (2). Despite its importance, the regulation of mtDNA gene expression in response to cellular and metabolic demands is only partly understood. The basal machinery responsible for transcription initiation in mammalian mitochondria is a three-component system (3), consisting of the mitochondrial RNA polymerase, mitochondrial transcription factor B2 (TFB2M), and mitochondrial transcription factor A (TFAM) (4). In addition to its role in transcription, TFAM also has a role in fully coating and packaging mtDNA into nucleoids (5). There have been several reports of factors implicated in stimulation of the basal transcription machinery, but there is as yet no consensus about the role of these putative additional transcription activators, as exemplified by the debate surrounding the role for the ribosomal subunit MRPL12 in transcription (3, 6). Transcription may also be regulated at the level of termination via the binding of mitochondrial transcription termination factor 1 (MTERF1) to a 28-bp region directly downstream of the two rRNA genes (7, 8). MTERF1 belongs to the large MTERF family with many members in metazoans and plants (9). In mammals, a total of four members are known and MTERF1, MTERF2, and MTERF3 have all been suggested to interact with the promoter region and stimulate (10, 11) or repress transcription initiation (12). The structures of MTERF1 (13, 14) and MTERF3 (15) have previously been solved and are composed of several repeated MTERF-motifs, each consisting of three α-helices forming a triangular-like structure. The MTERF-motifs form a half-doughnut–shaped, right-handed superhelix, where the concave side displays a positively charged path for nucleic acid interaction. Recently, a new role for a member of the MTERF family was revealed, as MTERF4 unexpectedly was shown to be essential for mitochondrial translation (16). MTERF4 forms a stoichiometric complex with NSUN4 (a 5-methylcytosine RNA methyltransferase) and is required for the recruitment of NSUN4 to the large ribosomal subunit to accomplish an essential, but still poorly defined, step in ribosomal biogenesis. Loss of this targeting has dramatic effects, mitochondrial ribosome biogenesis is stopped, thereby causing an effective halt of mitochondrial translation.

NSUN4 belongs to a family of RNA 5-methylcytosine (m5C) methyltransferases (MTases) present in all kingdoms of life (17). The crystal structures of the RNA m5C MTases RsmB and RsmF in prokaryotes (18, 19) display a conserved MTase domain flanked by variable N- or C-terminal extensions proposed to function as RNA-binding modules. The methyl donor S-adenosyl-L-methionine (SAM) is bound at the base of a positively charged cleft in the MTase domain near two conserved cysteins important for the methylation mechanism. The cleft is large enough for binding a specific stem loop in 16S ribosomal RNA (rRNA) to methylate specific sites. There are several examples demonstrating that methylation of rRNA is important for ribosome biogenesis. In yeast, the RNA m5C MTase Nop2p (20) and Nop8p (21, 22) are essential for assembly of the large ribosomal subunit. In mitochondria, TFB1M dimethylates two adenines in a conserved stem-loop at the 3′ end of 12S rRNA and this modification is essential for biogenesis of the small ribosomal subunit (23).

Here, we describe the structure of a heterodimeric complex between MTERF4 and NSUN4 at 2.9 Å resolution. MTERF4 consists of repeated MTERF-motifs and its carboxyl-terminal domain binds NSUN4 through conserved polar and hydrophobic interactions. There is a positively charged RNA binding path along the concave and convex sides of MTERF4 that extends into the active site of NSUN4, where SAM is present in

Author contributions: H.S., C.M.G., N.-G.L., and B.M.H. designed research; H.S. and B.M.H. performed research; H.S., B.H., and B.M.H. analyzed data; and H.S., B.H., C.M.G., N.-G.L., and B.M.H. wrote the paper.

The authors declare no conflict of interest.

*This Direct Submission article had a prearranged editor.

Freely available online through the PNAS open access option.

Data deposition: The atomic coordinates have been deposited in the Protein Data Bank, www.pdb.org (PDB ID code 4FP9).

[1]To whom correspondence may be addressed. E-mail: larsson@age.mpg.de or martin.hallberg@ki.se.

This article contains supporting information online at www.pnas.org/lookup/suppl/doi:10.1073/pnas.1210688109/-/DCSupplemental.

BIOCHEMISTRY

a conserved RNA m5C MTase active site. MTERF4 is thus likely to provide the sequence-specific RNA binding domain necessary for specific rRNA methylation by NSUN4. This unique function for a member of the large MTERF family of proteins makes it likely that at least some of the many homologs in plants and metazoans have similar functions.

Results and Discussion

Crystallization and Structure Determination. The protein complex of the mature, intramitochondrial forms of human MTERF4 (residues 48–381) and NSUN4 (residues 26–384) was purified and crystallized. The structure was determined by experimental phasing and the final model was refined to an R_{free} of 24.6%, calculated to 2.9 Å resolution (Table S1). The crystal contains four MTERF4–NSUN4 complexes per asymmetric unit, with a rmsd of 0.62 Å and 0.22 Å for MTERF4 and NSUN4, respectively; thus, there are no significant conformational variations between the four complexes within the asymmetric unit. The overall complex structure has an elongated shape with the dimension 45 × 47 × 122 Å (Fig. 1*A*). Upon solving the structure, it was apparent that the methyl donor SAM from the *Escherichia coli* overexpression host was bound in the active site (Fig. 1*B*).

Overall Structure of MTERF4. MTERF4 is an all α-helical protein that adopts a half-doughnut shape with a right-handed superhelical twist (Fig. 1*A*). The MTERF4 structure (residues 83–327) is composed of a total of six MTERF motifs comprising 18 α-helices that form four central MTERF-motifs, flanked by additional, partial MTERF-motifs at each terminus. In the N-terminal partial MTERF-motif, the third helix is missing, and in the C-terminal partial MTERF-motif, the middle helix is replaced by a long loop stretching out from the convex side of the protein. In addition to the MTERF motifs, MTERF4 contains two more α-helices at the C-terminus where the last helix (α18) makes an opposite turn, thus ending the half-doughnut shape. Residues 48–82 at the N terminus and residues 328–381 at the C terminus could not be modeled due to the weak electron density in these regions.

Structural Comparison of MTERF4 to Other MTERFs. The only structures showing significant structural similarity to the present MTERF4 structure were MTERF1 (13, 14) and MTERF3 (15).

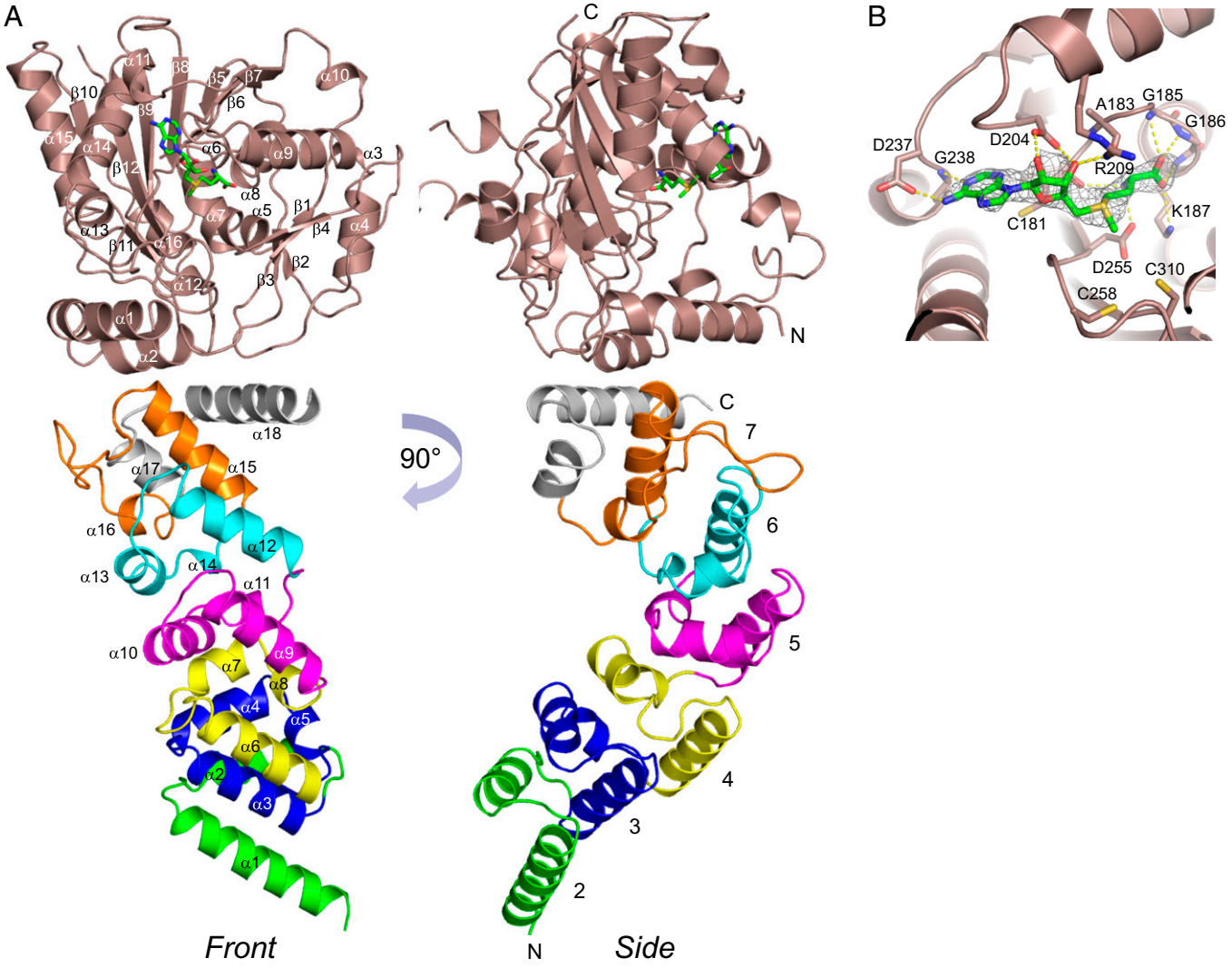

Fig. 1. Overall structure of the MTERF4–NSUN4 complex. (*A*) Front and side views of the MTERF4–NSUN4 complex are in cartoon representation with NSUN4 colored in dark salmon with SAM showed in stick mode (green). The MTERF motifs of MTERF4 are numbered (*side view*) as in ref. 15 and have the following color code: 2, green; 3, blue; 4, yellow; 5, magenta; 6, cyan; 7, orange. The additional motif of MTERF4 is in gray and the N- and C-terminals are indicated. The secondary structure elements are numbered (front view). (*B*) SAM binding site in NSUN4. Polar interactions between SAM and coordinating residues are indicated. The view is rotated for clarity. Electron density around SAM as calculated from density modified and fourfold averaged experimental phases contoured at 1.0 σ and shown in gray mesh.

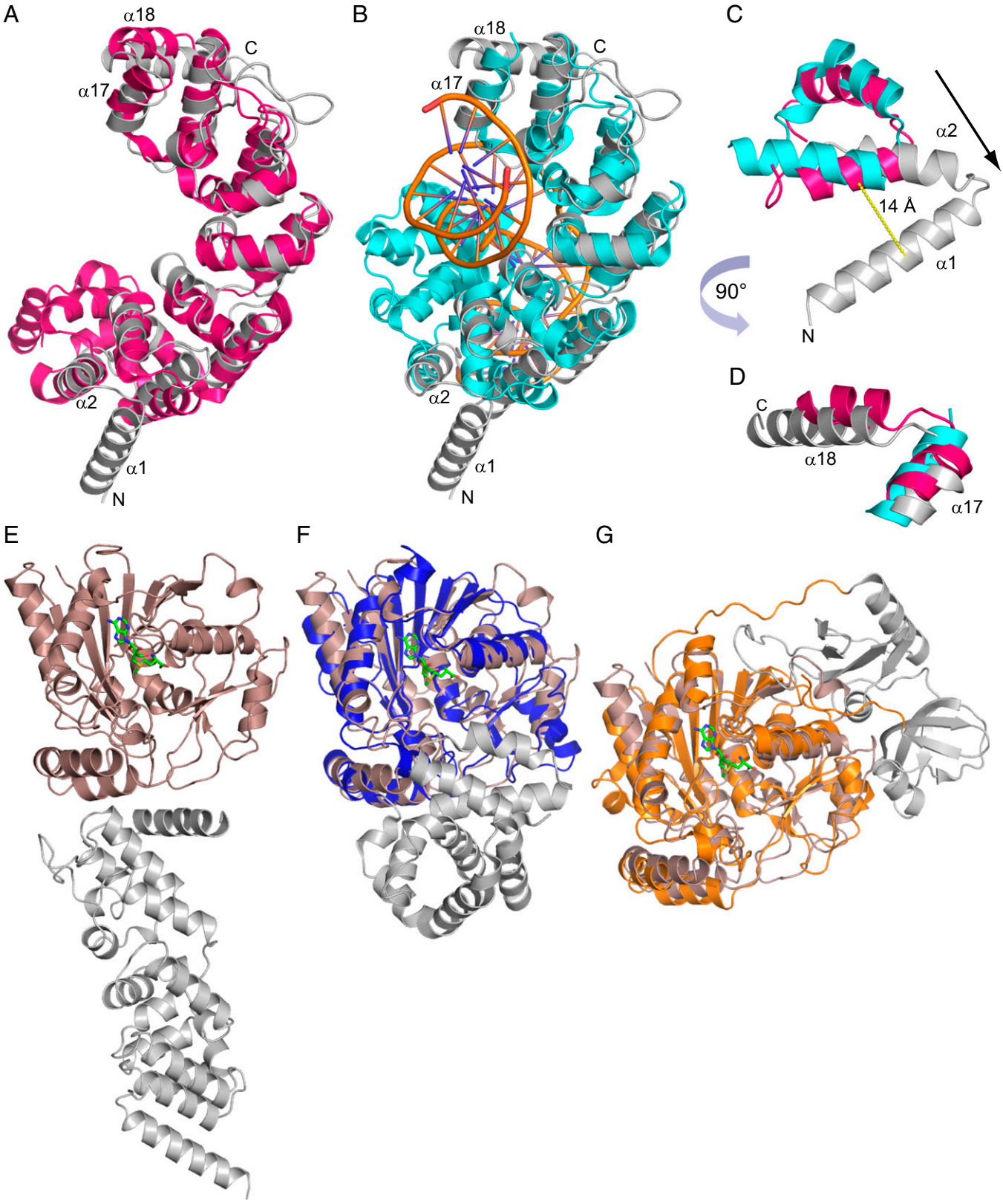

Fig. 2. Structural comparison of MTERF4 and NSUN4 with related structures. (*A*) Side view of MTERF4 (gray) superimposed with MTERF3 (PDB ID code 3M66) (15) colored in pink. (*B*) Superimposition of MTERF4 (gray) with MTERF1 (cyan) bound to DNA colored in orange (PDB ID code 3MVA) (14). (*C*) Shift of MTERF-motif 2. MTERF4, MTERF3, and MTERF1 are rotated 90° around the *y* axis compared with *A* and *B* (*back view*) with the same coloring scheme. (*D*) Comparison of MTERF4, MTERF3, and MTERF1 at the C-terminus. Back view with the same color scheme as in *A* and *B*. (*E*) Front view of the MTERF4–NSUN4 complex. NSUN4 is colored in dark salmon and MTERF4 in gray. (*F*) Superimposition of NSUN4 (dark salmon) with *E. coli* RsmB (PDB ID code 1SQF) (19) colored in blue, except for the eight-helix RNA-binding domain, which is colored in gray. (*G*) Superimposition of NSUN4 (dark salmon) with *TTH* RsmF (PDB ID code 3M6W) (18) colored in orange, except for the PUA-like RNA-binding domains, which are colored in gray. The structural alignment was performed using the secondary-structure matching method.

A structure-based sequence alignment (Fig. S1*A*) showed an evenly distributed conservation at the center of the proteins. In contrast, the N termini were highly divergent and the C-termini displayed similarity only between MTERF4 and MTERF3. A superposition of MTERF4 with MTERF3 gave an rmsd value of 3.21 Å using 186 Cα atoms (Fig. 2*A*), whereas MTERF1 gave an rmsd value of 3.37 Å using 167 Cα atoms (Fig. 2*B*). The similarities were most pronounced at the central part of the protein with larger deviations at the terminals. At the N-terminus, MTERF-motif 2 is shifted about 14 Å compared with MTERF1 and MTERF3 (Fig. 2*C*). The effect is a straighter path for the protein that breaks the half-doughnut shape created by the other MTERF motifs. There is a more pronounced curved shape of MTERF1 bound to DNA compared with apo-MTERF3

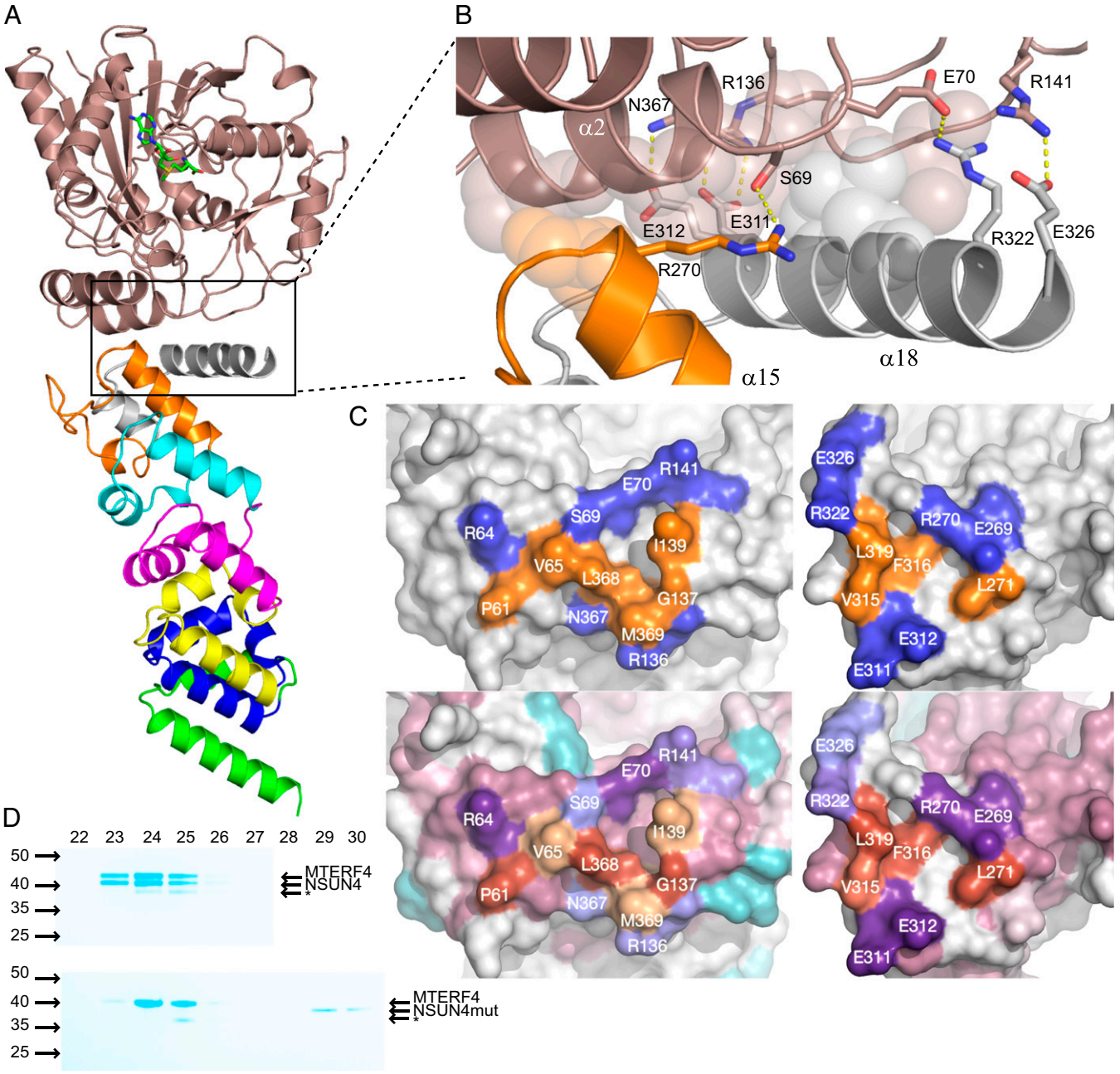

Fig. 3. MTERF4–NSUN4 binding interface. (*A*) Front view of the overall structure of the MTERF4–NSUN4 complex. (*B*) Blow-up of MTERF4–NSUN4 binding interface. Interacting polar residues are shown with sticks and hydrophobic residues as spheres. (*C*) Solvent-excluded surface representation of the interface region of NSUN4 (*Left*) and MTERF4 (*Right*). (*Upper*) Surface corresponding to residues forming hydrophilic interactions and residues forming hydrophobic interactions are shown in blue and orange, respectively. (*Lower*) Consurf (29) coloring based on sequence conservation in a set of sequences that is above 40% identical to either human NSUN4 or human MTERF4 (all vertebrates). The conservation-based coloring was combined with the interaction information (*Upper*). Dark violet: hydrophilic interaction, strongly conserved; light blue: hydrophilic interaction, not conserved; dark red: hydrophobic interaction, strongly conserved; beige: hydrophobic interaction, not conserved; pink: no interface interaction, conserved; turquoise: no interface interaction, strongly varying. (*D*) Mutation analysis of the MTERF4–NSUN4 interface. (*Upper*) Mixed MTERF4 and NSUN4 were subjected to gel filtration and peak fractions were separated on a SDS/PAGE gel and identified with MALDI-TOF MS. Arrows on the left indicate molecular masses according to standard and arrows on the right identified proteins. The band below NSUN4 (*) is a degradation product of MTERF4. (*Lower*) The same as in the upper panel, but a version of NSUN4 (NSUN4mut) mutated in the MTERF4–NSUN4 interface was used instead of NSUN4.

and apo-MTERF4 (Fig. 2*B*). However, it is probable that MTERF4 and MTERF3 will also obtain an increased curvature when bound to their respective putative RNA or DNA substrate, possibly displaying a nucleic acid-protein mutually induced fit (24). Furthermore, in contrast to MTERF1, both MTERF3 and MTERF4 have a loop instead of the central helix in MTERF-motif 7. Many important MTERF4–NSUN4 interface-forming residues are located in α18 of MTERF4 (Fig. 3 *B* and *C*). Interestingly, of those, only F316 is conserved in MTERF3 (Fig. S1*A*), whereas this helix is completely missing in MTERF1 (Fig. 2*D* and Fig. S1*A*); this finding would explain why MTERF4, and not other MTERFs, can recruit NSUN4 to the large ribosomal subunit in mitochondria. However, as MTERF3 also displays an α18 helix in a similar conformation as in MTERF4, it is possible that MTERF3 could form a complex with an unknown protein in a similar fashion as in the MTERF4–NSUN4 complex presented here.

Overall Structure of NSUN4. NSUN4 contains a typical RNA m5C MTase core domain and lacks variable N- or C-terminal extensions common for RNA recognition in other RNA m5C MTases (18, 19, 25) (Fig. 1*A*). NSUN4 (residues 39–384) is composed of 16 α-helices and 12 β-strands, where both α-helices and β-strands contribute to build up an active site cleft. The adenine ring of bound SAM is positioned in a mainly hydrophobic pocket with additional polar contacts to G238 and D237 (Fig. 1*B*). The ribose hydroxyl groups form hydrogen bonds to D204 and R209, whereas the methionine amino group forms contacts to the carbonyl group of C181 and D255. Furthermore, the carboxyl group of SAM is bound in a strongly basic pocket formed by the backbone amides of G185, G186, K187, and the N^Z of K187. The SAM donor methyl points toward the open cleft where two loops comprising the conserved cysteine residues C258 and C310 are located. These cysteines are important for the methyl transfer mechanism from SAM to the incoming RNA (17, 19). In this context, C310 in NSUN4 serves as a catalytic nucleophile, whereas C258 eases product release from the covalent enzyme-RNA intermediate.

Structural Comparison of NSUN4 to Other RNA m5C MTases. A search for structural homologs to NSUN4 using Dali (26) revealed significant matches to other RNA m5C MTases (18, 19, 25), thus enabling a structural-based sequence alignment between NSUN4 and the *E. coli* structural homologs RsmF and RsmB, as well as RsmF from *Thermus thermophilus* (*TTH*) (Fig. S1*B*). The highest sequence similarity was found at the central part of the protein, especially around the SAM binding active site. The structure database search also revealed similarity to human NSUN5 that belongs to the same family as NSUN4, although with a lower *Z*-score than for RsmF and RsmB (Table S2). We superimposed the structure of NSUN4 with RsmF and RsmB (Fig. 2 *E*–*G*). The rmsd for the structural superimpositions are 1.9 Å using 243 Cα atoms in RsmF from *E. coli*, 2.0 Å using 254 Cα atoms in RsmF from *TTH*, and 2.1 Å using 244 Cα atoms in RsmB from *E. coli* (18, 19, 25). In contrast to NSUN4, RsmF and RsmB contain RNA binding domains, which are located in different positions (Fig. 2 *F* and *G*). In contrast to RsmF, the RNA-binding domain of RsmB is in a similar location as MTERF4 in the MTERF4–NSUN4 complex (Fig. 2 *E*–*G*). Furthermore, the RNA-binding motif in RsmB is all α-helical as in MTERF4, and consists of two repeats that each contains four α-helices that can be structurally aligned. However, the arrangement of the α-helical repeats is entirely different in RsmB compared with MTERF4. In the active site, SAM and the conserved cysteins important for the methylation mechanism are almost in identical positions in NSUN4 compared with RsmF and RsmB (Fig. S2). The observation that an RNA recognition domain and an RNA m5C MTase catalytic domain are located in different proteins is not unique to the MTERF4–NSUN4 complex. Nop8p, a nuclear RNA m5C MTase homolog to NSUN4 in yeast, forms a complex with Nip7p that is essential for substrate recognition. Nip7p contains a pseudouridine synthase and archaeosine transglycosylase-domain that aids recruitment of Nop8p to the 27S ribosomal subunit. This recruitment is crucial for assembly of the 60S ribosome (21, 22).

MTERF4–NSUN4 Binding Interface. Both hydrophobic and polar interactions build up the MTERF4–NSUN4 binding interface (Fig. 3 *A*–*C* and Table S3). The MTERF4–NSUN4 interface buries 1,380 $Å^2$ of solvent-accessible surface area, in line with what is expected for a heterocomplex of this size (27).

The C-terminal part of the MTERF4 protein, primarily α18, interacts with NSUN4. In contrast, the distribution of interface-forming residues of NSUN4 is broader, stretching all of the way from α2 to the loop between β11 and β12. Four polar residues—E311, E312, R322, and E326—at both ends of α18 in MTERF4 form hydrogen bonds to R136, N367, E70, and R141 in NSUN4 (Fig. 3 *B* and *C*). In addition, a hydrogen bond is formed between R270 of MTERF4 and S69 of NSUN4. The central part of α18 in MTERF4 further contributes to interface stability through a number of hydrophobic residues building up a hydrophobic interface between the proteins (Fig. 3 *B* and *C* and Table S3). An additional hydrophobic interface is formed between α15 of MTERF4 and α2 of NSUN4. In NSUN4 and MTERF4, the hydrophilic interaction patches form a triangle with a central hydrophobic area in between (Fig. 3*C*). The majority of the interface-forming residues are conserved (Fig. 3*C*, Fig. S3, and Table S4), and in cases where residues are not conserved there are compensatory substitutions on the partner interface, indicating at least some level of coevolution. Interestingly, the key residue of this interface, L271, and the immediate sequence following it are conserved in MTERF3 (Fig. S1*A*). Along with the homology in the conformation and key sequence elements in α18, these findings point further toward a possible similarity in function between MTERF3 and MTERF4.

To validate the MTERF4–NSUN4 interface found in the crystal structure, we introduced four point mutations in NSUN4 to see if we could break the interaction with MTERF4. We selected two hydrophobic residues (V65R and I139R) and two polar residues (R136A and R141A), because both types clearly contribute to the interaction. The mutated NSUN4 (NSUN4mut) or NSUN4 was added to MTERF4 and subjected to gel filtration. MTERF4–NSUN4 forms a stoichiometric complex that migrate together over the gel-filtration column (Fig. 3*D*, *Upper*). In contrast, NSUN4mut cannot bind MTERF4, which instead forms an apparent homodimer. Thus, MTERF4 and NSUN4mut migrate in base-line separated peaks (Fig. 3*D*, *Lower*), meaning that the interface we observe in our heterocomplex crystal structure is genuine.

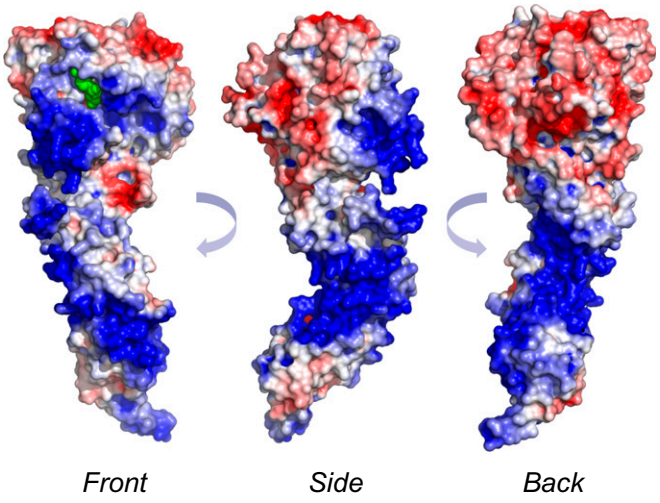

Fig. 4. Surface representation of the MTERF4–NSUN4 complex. Front, side, and back views of the molecular surface is colored by the local electrostatic potential (blue, +5 kT; red −5 kT). SAM is shown with green spheres.

RNA Binding Surface. The MTERF4–NSUN4 complex displays a highly asymmetrical surface charge distribution (Fig. 4). The backside of NSUN4 is widely negatively charged and has the same orientation as the strongly positively charged concave side of MTERF4 (Fig. 4, *Right*). The positively charged surface forms a path along MTERF4 that continues on the side (Fig. 4, *Center*) all of the way around to the convex side of the protein (Fig. 4, *Left*). There, the path continues along MTERF4, reaching the front side of NSUN4, where it approaches the SAM-bound active site. Thus, both proteins contribute to the highly positively charged path. We interpret the positively charged surface along the MTERF4–NSUN4 complex as a very likely RNA binding path. It is conceivable that MTERF4 contacts a sequentially different part of rRNA than NSUN4 does and thereby works to position NSUN4 at the site of modification. This finding is similar to what was recently observed in the EM structure of KsgA from *E. coli* bound on the 30S subunit (28). In that case, the N- and C-terminal domains contact sequentially distant parts of rRNA.

Interestingly, only the beginning of the acidic C-terminal tail in MTERF4 is visible in the structure: it is located in a position where it could prevent the RNA from taking the wrong direction or even help push it into the active site.

Conclusions

The presented structure of the MTERF4–NSUN4 complex at 2.9 Å resolution demonstrates that specific hydrophobic and polar residues in both proteins hold the complex together. The observation that the mutation of four of these interacting residues completely disrupts complex formation on size-exclusion chromatography validates the structural predictions on how MTERF4 and NSUN4 interact. In addition, bioinformatic analyses show high conservation of the hydrophobic and polar residues at the subunit interface, thus further validating the mechanism for complex formation. Strikingly, there is a long positively charged path on the surface of the structure, which extends from the concave to the convex side of MTERF4 and then further along NSUN4 into the catalytic site where SAM is bound. This path likely represents the RNA binding capacity necessary to accomplish specific m5C modification of mitochondrial rRNA of the large mitochondrial ribosomal subunit. The structure not only reveals a molecular basis for the highly conserved function of MTERF4 in ribosomal biogenesis, but also predicts that more members of the large MTERF family in plants and metazoans may have a similar function, especially because carboxyl-terminal sequence features similar to the ones found in MTERF4 are present in several members.

Methods

Cloning and Purification of the MTERF4–NSUN4 Complex. Recombinant MTERF4 and NSUN4 were heterologously coexpressed and purified as detailed in *SI Methods*.

Mutation Analysis of the MTERF4–NSUN4 Interface. Four point mutations, V65R, R136A, I139R, R141A, were introduced in NSUN4 by site directed mutagenesis. The mutated form of NSUN4, native NSUN4 and MTERF4 were expressed, purified and subjected to gel filtration, as specified in *SI Methods*.

Crystallization and Structure Solution. Native and selenomethionine (Se-Met) crystals of the MTERF4–NSUN4 complex were grown by the hanging-drop vapor-diffusion method in a condition specified in *SI Methods*. A Ta_6Br_{12} derivatized crystal and two Se-Met containing crystals were used to collect anomalous data to solve the structure with multiple isomorphous replacement. Details of phasing, model building, and refinement are provided in *SI Methods* and statistics are listed in Table S1.

ACKNOWLEDGMENTS. We thank Emily Hoberg for producing cells containing baculovirus-expressed wild-type MTERF4. The crystallographic experiments were performed on the X06SA beam-line at the Swiss Light Source, Paul Scherrer Institut, Villigen, Switzerland. The study was supported by Swedish Research Council Grant 2009-4848 (to C.M.G.) and Grants 2010-5059 and 2011-6510 (to B.M.H.); a grant from the Swedish Cancer Foundation (to C.M.G.); and by a joint European Research Council Advanced Investigator grant (to N.-G.L and C.M.G.). Data collection was partly funded by the European Community's Seventh Framework Programme (FP7/2007-2013) under Grant 226716.

1. Park CB, Larsson NG (2011) Mitochondrial DNA mutations in disease and aging. *J Cell Biol* 193:809–818.
2. Falkenberg M, Larsson NG, Gustafsson CM (2007) DNA replication and transcription in mammalian mitochondria. *Annu Rev Biochem* 76:679–699.
3. Litonin D, et al. (2010) Human mitochondrial transcription revisited: Only TFAM and TFB2M are required for transcription of the mitochondrial genes in vitro. *J Biol Chem* 285:18129–18133.
4. Falkenberg M, et al. (2002) Mitochondrial transcription factors B1 and B2 activate transcription of human mtDNA. *Nat Genet* 31:289–294.
5. Kukat C, et al. (2011) Super-resolution microscopy reveals that mammalian mitochondrial nucleoids have a uniform size and frequently contain a single copy of mtDNA. *Proc Natl Acad Sci USA* 108:13534–13539.
6. Surovtseva YV, et al. (2011) Mitochondrial ribosomal protein L12 selectively associates with human mitochondrial RNA polymerase to activate transcription. *Proc Natl Acad Sci USA* 108:17921–17926.
7. Daga A, Micol V, Hess D, Aebersold R, Attardi G (1993) Molecular characterization of the transcription termination factor from human mitochondria. *J Biol Chem* 268: 8123–8130.
8. Kruse B, Narasimhan N, Attardi G (1989) Termination of transcription in human mitochondria: Identification and purification of a DNA binding protein factor that promotes termination. *Cell* 58:391–397.
9. Linder T, et al. (2005) A family of putative transcription termination factors shared amongst metazoans and plants. *Curr Genet* 48:265–269.
10. Martin M, Cho J, Cesare AJ, Griffith JD, Attardi G (2005) Termination factor-mediated DNA loop between termination and initiation sites drives mitochondrial rRNA synthesis. *Cell* 123:1227–1240.
11. Wenz T, Luca C, Torraco A, Moraes CT (2009) mTERF2 regulates oxidative phosphorylation by modulating mtDNA transcription. *Cell Metab* 9:499–511.
12. Park CB, et al. (2007) MTERF3 is a negative regulator of mammalian mtDNA transcription. *Cell* 130:273–285.
13. Jiménez-Menéndez N, et al. (2010) Human mitochondrial mTERF wraps around DNA through a left-handed superhelical tandem repeat. *Nat Struct Mol Biol* 17:891–893.
14. Yakubovskaya E, Mejia E, Byrnes J, Hambardjieva E, Garcia-Diaz M (2010) Helix unwinding and base flipping enable human MTERF1 to terminate mitochondrial transcription. *Cell* 141:982–993.
15. Spåhr H, Samuelsson T, Hällberg BM, Gustafsson CM (2010) Structure of mitochondrial transcription termination factor 3 reveals a novel nucleic acid-binding domain. *Biochem Biophys Res Commun* 397:386–390.
16. Cámara Y, et al. (2011) MTERF4 regulates translation by targeting the methyltransferase NSUN4 to the mammalian mitochondrial ribosome. *Cell Metab* 13: 527–539.
17. Reid R, Greene PJ, Santi DV (1999) Exposition of a family of RNA m(5)C methyltransferases from searching genomic and proteomic sequences. *Nucleic Acids Res* 27: 3138–3145.
18. Demirci H, et al. (2010) Multi-site-specific 16S rRNA methyltransferase RsmF from *Thermus thermophilus*. *RNA* 16:1584–1596.
19. Foster PG, Nunes CR, Greene P, Moustakas D, Stroud RM (2003) The first structure of an RNA m5C methyltransferase, Fmu, provides insight into catalytic mechanism and specific binding of RNA substrate. *Structure* 11:1609–1620.
20. King M, Ton D, Redman KL (1999) A conserved motif in the yeast nucleolar protein Nop2p contains an essential cysteine residue. *Biochem J* 337:29–35.
21. Zanchin NI, Goldfarb DS (1999) Nip7p interacts with Nop8p, an essential nucleolar protein required for 60S ribosome biogenesis, and the exosome subunit Rrp43p. *Mol Cell Biol* 19:1518–1525.
22. Zanchin NI, Roberts P, DeSilva A, Sherman F, Goldfarb DS (1997) *Saccharomyces cerevisiae* Nip7p is required for efficient 60S ribosome subunit biogenesis. *Mol Cell Biol* 17:5001–5015.
23. Metodiev MD, et al. (2009) Methylation of 12S rRNA is necessary for in vivo stability of the small subunit of the mammalian mitochondrial ribosome. *Cell Metab* 9:386–397.
24. Seif E, Hallberg BM (2009) RNA-protein mutually induced fit: Structure of *Escherichia coli* isopentenyl-tRNA transferase in complex with tRNA(Phe). *J Biol Chem* 284: 6600–6604.
25. Hallberg BM, et al. (2006) The structure of the RNA m5C methyltransferase YebU from *Escherichia coli* reveals a C-terminal RNA-recruiting PUA domain. *J Mol Biol* 360: 774–787.
26. Holm L, Kääriäinen S, Rosenström P, Schenkel A (2008) Searching protein structure databases with DaliLite v.3. *Bioinformatics* 24:2780–2781.
27. Jones S, Thornton JM (1996) Principles of protein-protein interactions. *Proc Natl Acad Sci USA* 93:13–20.
28. Boehringer D, O'Farrell HC, Rife JP, Ban N (2012) Structural insights into methyltransferase KsgA function in 30S ribosomal subunit biogenesis. *J Biol Chem* 287: 10453–10459.
29. Ashkenazy H, Erez E, Martz E, Pupko T, Ben-Tal N (2010) ConSurf 2010: Calculating evolutionary conservation in sequence and structure of proteins and nucleic acids. *Nucleic Acids Res* 38(Web Server issue):W529–W533.